Technical Evaluation of Glauconies as Alternative Potassium Fertilizer from the Salamanca Formation, Patagonia, Southwest Argentina

Corina Franzosi,[1,4] Liliana N. Castro,[1,2] and Ana María Celeda[3]

The aim of this work was to evaluate the Salamanca Formation greensands as an alternative potassium fertilizer to KCl. Glauconitic pellets from this formation tend to naturally concentrate in 600–250 μm (BS 250) and 250–125 μm (BS 125) fractions. After dry sieving and magnetic separation, these fractions were used for chemical, lixiviation, and specific surface analyses and agronomic evaluations. Two concentrated products were obtained: GL250c (600–250 μm) and GL125c (250–125 μm) representing 40.9 % of total sample. GL250c contains 2.97 % K_2O, and GL125c contains 4.05 % K_2O, representing 27 and 60 % increase in K-content compared to the bulk sample. Grain size of both concentrates decreased significantly through lixiviation tests. Potassium release curves from lixiviation waters show that K-liberation from GL250c was more effective in the first 15 days but decreased after that whereas liberation from GL125c continued to increase after 15 days probably due to higher K-content (36 % higher than GL250c). Specific area could have influenced liberation rates because after leaching it increased 27 % for the finer fraction and by only 16 % for the coarser one. From agronomic assays, measured over 75 days with five harvests, the first four harvests yield best results from KCl probably due to fast K-liberation rates from the salt. However, after overall harvests, fertilization efficiency using either GL250c or GL125c was very similar to and slightly higher than KCl fertilization. As equivalent results were found using either GL250c or GL125c, sieving to obtain these fractions seems not necessary. The results indicate that greensands from the Salamanca Formation are effective slow release alternative K source for fertilizers with low cost of production and treatment compared to operation costs required for mining K soluble salts at depth.

KEY WORDS: Greensands, Alternative potassium fertilizer, Magnetic concentration process, Salamanca Formation, Argentina.

[1]Departamento de Ciencias Geológicas – IGEBA, Facultad de Ciencias Exactas y Naturales, Universidad de Buenos Aires, Ciudad Universitaria, Pabellón II, Intendente Güiraldes 2160, C1428EHA, Ciudad Autónoma de Buenos Aires, Argentina.

[2]Departamento de Ingeniería Agricola y uso de la tierra, Facultad de Agronomía, Universidad de Buenos Aires, Av. San Martín 4453, C1417DSE, Buenos Aires, Argentina.

[3]INTEMIN – SEGEMAR, Av. General Paz 5445, Ed. 14, General San Martín, B1650KNA, Buenos Aires, Argentina.

[4]To whom correspondence should be addressed; e-mail: cfranzosi@gmail.com

INTRODUCTION

Potassium is one of the essential nutrients together with phosphorous and nitrogen for crops. Year by year, the demand for fertilizers increases as world population continues to grow. The demand for K-fertilizer is projected to grow at an annual rate of 3 % from 2012 to 2017, reaching 37.4 Mt K_2O in 2017 (Heffer and Prud'homme 2013). Nowadays, soluble salts (KCl) dominate the K-fertilizer market. Still, alternative K-fertilizers are of interest as local sources for selective organic crops.

Glaucony, usually called *greensands*, is loose to consolidated glauconite-rich sands that have been used as natural fertilizers, especially in forage crops, for over 100 years (Dooley 2006). Their peak usage was reached before World War II, when it was replaced by KCl because of higher K-content. In Denmark, greensands have been used as slow acting K-fertilizer by direct application. Large indigenous resources of glauconitic sandstones (over 3,000 million tons), considered as an alternative potash source, have been identified in India (TIFAC 2009). At present, Brazil is trying to decrease its dependency on K-salt imports, using 8–10 % K_2O *Verdete*, a K- and Fe-rich slate rock (metamorphosed greensands) found in Minas Gerais. Amazons Cerrado Verde Potash Project (2012) proposes to produce slow-release, nonchloride, and multi-nutrient fertilizers from these rocks (http://www.amazonplc.com). In West Australia's Perth Basin and in New Zealand, prospects of glauconitic sands are being developed at present day (www.potashwest.com.au, http://www.glauconitenz.co.nz). In addition, the potential development of marine deposits of potassic and phosphatic minerals offshore in Southern Africa has been evaluated for the manufacture of fertilizer (Coles et al. 2002). Castro and Tourn (2004) described glaucony deposits in Patagonia (Argentina) and suggested the use of glauconitic and phosphatic sediments as direct spread fertilizers. Castro et al. (2008) and Franzosi (2009) presented results where magnetically upgraded 125–250 μm grain size glauconies caused significant improved growth in seedlings at laboratory tests. Castro et al. (2010) showed results of agronomic assays, comparing the efficiency of Patagonian greensands with a traditional potassium fertilizer (KCl).

Greensands are still being used nowadays in organic crops such as berries. The analysis of potash commodity (2012) by the United States Geological Survey (http://minerals.usgs.gov/minerals/pubs/commodity/potash/mcs-2013-potas.pdf) indicates glaucony (greensand) as substitute of traditional fertilizer restricted to locations near the exploitation fields. One of the advantages of using greensands is that glauconite lacks of Cl, avoiding early salinization problems that may occur when using traditional fertilizers (KCl) produced from soluble salts such as kainite, sylvite, and carnallite, which may entail underground water contamination. An additional advantage of glaucony is its use as K^+ exchanger for heavy metals and ammoniac in polluted water remediation (Hao and Tsai 1987; Abd El-Rahman

2006). Moreover, Levchenko et al. (2008) proposed multifunctional purposes for Russian glauconites mainly for agricultural, land reclamation on wastes, and tailings pits.

The term glaucony was suggested by Odin and Matter (1981) when referring to greensands and glauconite for strictly referring to the K-aluminosilicate. Glauconite is a K-rich monoclinic micaceous mineral of defined chemical composition $(K, Ca, Na)_{\sim 1.6}(Fe^{3+}, Al, Mg, Fe^{2+})_{4.0}(Si_{7.3}Al_{0.7})_4O_{20}(OH)_4$. It presents low isomorphic substitution in the silica tetrahedrons and a dominant iron substitution in the alumina octahedrons.

According to McRae (1972), glauconite is *sensu lato* a random interstratification of nonexpanding 10 Å and expanding montmorillonitic layers. The amount of expandable layers may be over 50 %, but the name glauconite is sensu stricto restricted to varieties with less than 10 % expandable layers. The variation in the amount of expandable layers explains the differences in chemical composition (especially K-content), thermal characteristics, cation exchange capacity, color, refractive index, and specific gravity. High potassium cation (K^+) content between layers is common. Glauconite is found associated particularly with marine transgressions. Morphologically, glauconite grains are believed to form as casts, fecal pellets, or by accretionary growth. It is typically found as rounded pellets or grains with size similar to sands (Dooley 2006). Nevertheless, their morphology can be modified by subsequent re-working. Greensands have no use as a conventional fertilizer at present, but soils formed on glauconitic parent materials are notable for their fertility. Weathering carries the loss of K from glauconite to produce a montmorillonitic or vermiculitic product with the release or oxidation of structural Fe. Consequently glauconite grains can be converted to goethite. Iron content in glauconite structures gives paramagnetic properties to this mineral allowing the use of magnetic treatments for its concentration. A positive correlation exists between Fe- and K-content of glauconite.

Many researchers have referred to the stratigraphic significance of glauconitic levels as low sedimentation rate indicators and condensed sections under shallow marine conditions considering them as key elements in sequence stratigraphy (Amorosi 1995, 1997; Amorosi and Centineo 1997; Kitamura 1998; Banerjee et al. 2008; Chattoraj et al. 2009), but few publications report their characterization as industrial mineral for crop fertilization.

Technical Evaluation of Glauconies

The aim of this work is to study the use of Salamanca Formation glauconies for agronomic purposes considering their mineralogical, chemical, and textural characteristics. Additionally, preliminary evaluations on the possibilities of obtaining a commercial K-product for small scale agriculture developments by simple dry sieving and magnetic concentration techniques were carried out.

Greensands in the Salamanca Formation

Greensands, moderately sorted and weakly consolidated sands, appear in the *Banco Verde* or green strata within the top section of the Salamanca Formation. They are exposed intermittently within a 5,300 km^2 belt at surface and subsurface levels, 15 m average width and 2.5 % K_2O cut off content in continental land representing 2,800 Mt inferred resources (Castro and Soreda 2009). Greensands from Estancia Los Laureles in Chubut Province, Patagonia (45°33′40″ S, 68°13′40″ W) were used for this experimental research (Fig. 1).

MATERIALS AND METHODS

A representative sample of 50 kg was extracted from a 15-m long trench in the *Banco Verde* of the Salamanca Formation in Estancia Los Laureles, south Chubut Province, Patagonia (Argentina). The elemental composition of the sample was determined from chemical assays carried out on a stabilized sample at 105–110 °C, and lithium tetraborate was used as flux during automatic merging before analysis of major elements by X-ray fluorescence, wavelength dispersive. Certified reference materials were used for calibration and validation.

Sample granulometric distribution was obtained by dry standard sieving procedures using ASTM sieves. The cumulative mass curve is mathematically modeled with the internal hyperbolic tangent function $F(x) = \text{Tanh}[(x/p)^n]$ where x is particle diameter in μm, n is form factor, and the parameter p is parameter $D_{76\%}$ which is the grain diameter relative to which 76 % of the sample is finer. For clearer and better sedimentological characterization of the sample, statistical distribution parameters are calculated using the information provided by cumulative grain distribution curve, following Folk and Ward (1957) logarithmic graphical measures and using McManus (1988) terminology.

Two granulometric fractions, 600–250 μm (BS 250) and 250–125 μm (BS 125), were selected for all analyses as glauconite appears to be naturally concentrated in them. Coarser (>600 μm) and finer (<125 μm) fractions were left apart due to their low wt% in the total sample.

An Eriez 3 high intensity dry magnetic separator provided with NdBFe permanent magnets, producing a magnetic field between 15,000 and 20,000 Gauss, was used to concentrate glauconitic pellets on the 600–250 and 250–125 μm granulometric fractions. The magnetic roll retained magnetic particles, in this case mainly glauconitic pellets, from the feed stream leaving a ''non magnetic tailing.'' The magnetic product was reprocessed in order to increase the magnetic concentration. This purified product was labeled as ''magnetic concentrate.'' The remaining product from the second separation was identified as ''middling.'' Metallurgical balances were calculated for each granulometric fraction to evaluate the performance of the magnetic separation process. All products were analyzed by X-ray fluorescence. Correlations of wt% of K_2O with wt% of Al_2O_3, Fe_2O_3, and MgO were graphed.

Measurements of surface area of magnetic concentrates were carried out using a Micromeritics Gemini V sorptometer, and samples were previously degassed for 2 h after heating at 100 °C at atmospheric pressure under ultrapure N_2 steam. The contribution of external grains area and micropores was mathematically estimated from N_2 absorption–desorption isotherms. EDAX semi-quantitative analysis within zones of different colors and texture on selected grains were performed with an environmental scanning electron microscope Philips XL30.

For analyzing the agronomic effectiveness of the Salamanca Formation greensands, the 600–250 μm (GL250c) and 250–125 μm (GL125c) magnetically concentrated fractions were tested and compared with KCl fertilization (potash) and a control sample not fertilized with K. Agronomic tests were carried out in 8–10 cm height seedlings containing 7 kg of acidic soil (pH 4.9) with 10 g of grass seeds (*Festuca rubra* 47 %, *Poa trivialis* 23 %, *Lolium perenne* 18 %, and *Lolium multiflorum* 12 %) per seedling. All seedlings were fertilized with standard doses of urea, equivalent to 25 kg/ha and diammonium phosphate (DAP) equivalent to 150 kg/ha following Castro et al. (2010). For K-fertilization comparisons, three treatments were carried out with same initial K-content in equivalent
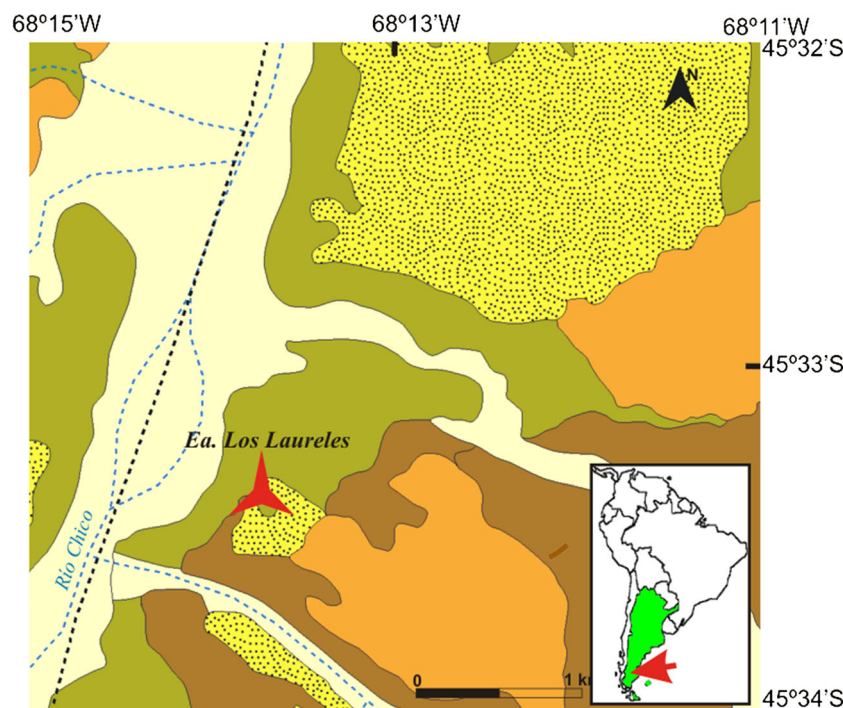
Fig. 1. Simplified geological map (modified from Franzosi 2009) showing sampling site.

%K$_2$O and one control sample: (1) control sample, (2) KCl (0.03 g/soil kg), (3) GL250c (5.3 g/soil kg), and (4) GL125c (7.3 g/soil kg). Five successive harvests were carried out at 15, 30, 45, 60, and 75 days. After each harvest, the soil was refertilized with DAP and urea, completely mixed and reseeded with the same amount of seeds. Moderate watering was applied. The aerial biomass collected at each harvest was weighed after two dryings: 65 °C and subsequently at 90 °C. The K$_2$O content incorporated by the grass during growth was analyzed by inductively coupled plasma atomic emission spectrometry (ICP-AES) on grass ashes obtained after calcination at 550 °C followed by acid digestion at controlled temperature.

In addition, for leaching analyses, 5 g of GL250c and 5 g of GL125c magnetically concentrated fractions were placed in five plastic tubes, and bi-distilled water was added to fill only the porous space. The tubes remained under controlled 60–63 % moisture atmosphere (the same moisture as supposed in the soil during agronomic tests). After 5 days, the possible "leached" elements were recovered by two washing-centrifuging steps in the first tube. The procedure was repeated after 13 days with the second tube, and after 21, 37, and 54 days with the third, fourth, and fifth tubes, respectively. In the collected washing liquids, K and Fe were analyzed by atomic absorption spectrometry and Al by ICP-AES. The variation in the particles size distribution of the original samples after leaching was determined by standard sieving of the five remaining solids previously dried at 100 °C.

RESULTS AND DISCUSSION

The granulometric analyses on greensands show unimodal distribution with mode in the 250–125 μm fraction corresponding to fine sands (Fig. 2). Using
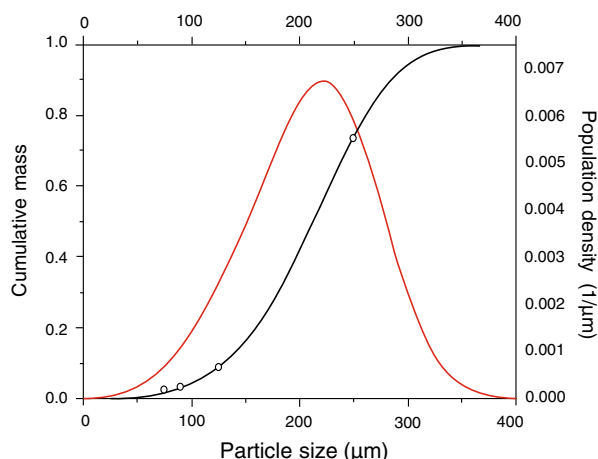
Fig. 2. Grain size distribution and cumulative mass curves for the Salamanca Formation greensands from Estancia Los Laureles, Patagonia, Argentina.

distribution parameters from Folk and Ward (1957), logarithmic graphical measures are presented in Table 1. The results showed a median diameter of 2.23 φ (213 µm), mean diameter of 2.28 φ (210 µm), standard deviation (σ_1) of 0.44, skewness of 0.27, and kurtosis of 1.10. The mean particle size corresponds to fine sands in 125–250 µm fraction according to granulometric intervals selected for this work. Values of one standard deviation about the mean, according to Folk and Ward (1957) and McManus (1988), correspond to well sort sediment supporting the observed pronounced unimodal distribution (Fig. 2). Additionally, the positive skewness value (0.27) reflects prevalence of coarser particle sizes and a fine grained tail. The kurtosis value (1.10) corresponds to a mesokurtic–leptokurtic curve, which matches with is in agreement with the other parameters.

The fine sands are mainly composed of quartz, glauconite (light–dark greenish black), and volcanic glass shards, plagioclase, altered K-feldspars (orthoclase), volcanic lithic fragments, and phosphatic pellets. Heavy minerals are less than 1 % and include pyroxenes (enstatite and augite), amphiboles (brown and green hornblende), goethite, magnetite, and biotite (Fig. 3). Glauconitic grains tend to concentrate within the 600–250 and 250–125 µm granulometric fractions. They mainly present lobate morphologies and light to dark green color with abundant cracks. Tourn et al. (2008) indicated that, based on X-ray diffraction, the mineralogical composition of glauconitic pellets includes

glauconite, illite-montmorillonite, and Na–Ca nontrolite.

The magnetic concentrates GL250c and GL125c represent 40.9 % of the bulk sample (Table 2). Sample elemental composition (Table 3) revealed that the bulk samples contain 2.34 and 2.54 % K_2O distributed in BS 250 and BS 125, respectively, and 2.97 and 4.05 % K_2O distributed in GL250c and GL125c, respectively. These indicate that magnetic concentration can enrich the K-content of bulk samples by 27–60 %. The results also show that magnetic concentration is useful for enriching the K-content of greensands, because they contain paramagnetic glauconitic pellets.

High SiO_2 values of 78.3 and 76.5 % in BS 250 and BS 125, respectively and 70.2 and 64.4 % in GL250c and GL125c, respectively, plus the absence of carbonatic minerals are in agreement with the data of Tourn et al. (2008), who suggest that glauconization could have been derived from a siliciclastic precursor. This hypothesis also helps to the positive correlations of K_2O with Al_2O_3, Fe_2O_3, and MgO, which further suggest simultaneous incorporation of these major elements in an incipient stage of glauconitization (Fig. 4).

Lixiviation tests indicated that both GL250c and GL125c underwent significant decrease in grain size (Fig. 5). GL250c was reduced to 70 wt% during the first 13 days of lixiviation and that wt% became constant in the successive harvests. Its breakdown released 45 wt% of 250–125 µm grain size particles and another 25 wt% of fractions 125–90 and <90 µm. In further harvests, no changes were observed in the 600–250 µm fraction. The wt% of 250–125 and 125–90 µm fractions continued to decrease at very slow rates resulting in an increase in wt% the <90 µm fraction. However, GL125c underwent a 40 wt% reduction in the first 13 days and continued to reduce at slower rates up to 50 wt% of its original weight. Accompanying this reduction, the 125–90 µm fraction reached 20 wt% in the first 13 days, and this became constant the following harvests, while the <90 µm fraction also reached 20 wt% in the first 13 days but continued to increase as the 250–125 µm fraction kept decreasing.

Specific area analyses revealed that GL250c showed 36 % higher specific area compared to GL125c and almost double amount of micropores. As lixiviation advanced, both samples underwent an increase in specific surface as grains broke down during lixiviation. Nevertheless, GL125c showed

Table 1. Statistical distribution parameters for the Salamanca Formation greensands from Estancia Los Laureles following the Folk and Ward (1957) logarithmic graphical measures and the McManus (1988) nomenclature

Parameters	Values	
Median diameter (Md)	2.23 φ	
Mean diameter (x)	2.28 φ	
Sorting (σ)	0.44 φ	Well sorted
Skewness (Sk1)	0.27	Positive asymmetry
Kurtosis (K_G)	1.10	Mesokurtic–leptokurtic

Values are given in φ according to Wentworth (1922)
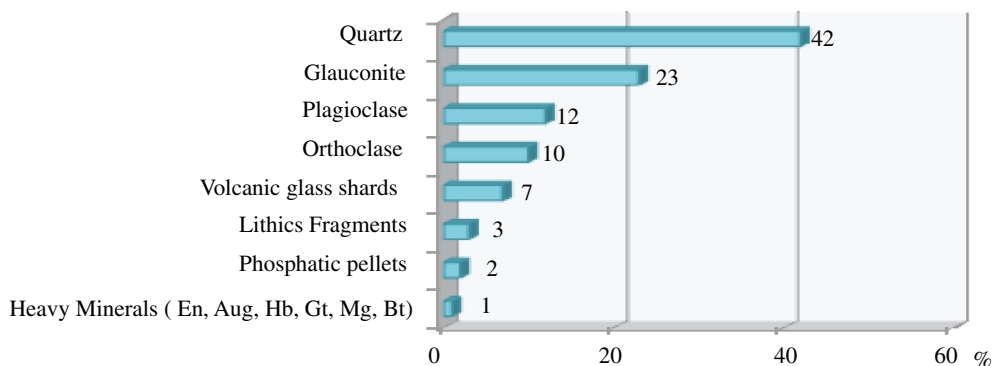
Fig. 3. Representative mineralogical composition of the Salamanca Formation greensands from Estancia Los Laureles, Patagonia, Argentina. *En* enstatite, *Aug* augite, *Hbl* hornblende, *Gt* goethite, *Mg* magnetite, *Bt* biotite.

Table 2. Granulometric distribution of total sample and magnetic and nonmagnetic products for 600–250, 250–125, and 125–90 μm granulometric fractions

Grain size (μm)	Magnetic separation products	Wt% within bulk sample	Wt% Mag and Non Mag per magnetically treated fraction	Wt% within product
>600	nmt	3.9		nmt
600–250	Non Mag	22.2	10.2	46.3
	Mag (GL250c)		11.9	53.7
250–125	Non Mag	65.4	36.4	55.7
	Mag (GL125c)		29.0	44.3
125–90	Non Mag	5.5	2.9	87.1
	Mag (GL90c)		0.7	12.9
90–74	nmt	0.8		nmt
<74	nmt	2.2		nmt
Total	nmt	100		nmt

higher relative increase in specific area of 27 %, while GL250c underwent 16 % increase.

Specific area tended to increase with lixiviation as grain size decreases. In addition, the decrease in micropores percentage during water leaching indicates that cracks are first attacked, and this could explain the breakdown of the pellets during lixiviation increasing the surface susceptible to chemical attack. Similar results were reported by Loveland (1981), who detected changes in the color of glaucony and intensive grain disaggregation during weathering. These are consistent with changes in textural characteristics of different glauconitic clays after acid leaching due to acid degradation and intensive acid penetration into grains (Srasra and Trabelsi-Ayedi 2000; Hassan and El-Shall 2004).

Potassium release curves were graphed using % K-content in lixiviation waters (Fig. 6). Potassium

Table 3. Chemical analyses (X-ray fluorescence) for products obtained after magnetic separation of 600–250 and 250–125 μm fractions

Grain size:	600–250 μm				250–125 μm			
Products	Mag (GL250c)	Mid	Non Mag	Bulk sample (BS 250)	Mag (GL125c)	Mid	Non Mag	Bulk sample (BS 125)
Wt%	53.7	20.5	25.8	100	44.3	14.2	41.5	100
SiO_2	70.2	81.4	88.7	78.25	64.4	79.7	85.7	76.46
Al_2O_3	9.75	8.35	6.11	8.33	11.9	10.2	8.4	10.01
Fe_2O_3	10.4	3.69	1.07	6.14	11.9	3.24	1.16	5.67
TiO_2	0.32	0.29	0.12	0.25	0.76	0.45	0.16	0.44
P_2O_5	0.08	0.08	0.04	0.07	0.08	0.06	0.03	0.05
MnO	0.08	0.04	0.01	0.05	0.03	0.02	0.01	0.02
CaO	0.98	1.21	1	1.03	0.87	1.34	1.57	1.26
MgO	0.38	0.17	0.07	0.24	0.65	0.22	0.12	0.34
K_2O	2.97	2.22	1.43	2.34	4.05	2.15	1.39	2.54
Na_2O	0.24	0.3	0.3	0.27	0.14	0.33	0.35	0.26
SO_3	0.03	0.02	0.01	0.02	0.01	0.01	0.01	0.01
LOI	4.26	2.01	0.9	2.75	4.97	2.03	0.89	2.65

nmt Not magnetically treated, *Mag* final magnetic concentrate, *Mid* Middlings, *Non Mag* non magnetic product after first magnetic concentration
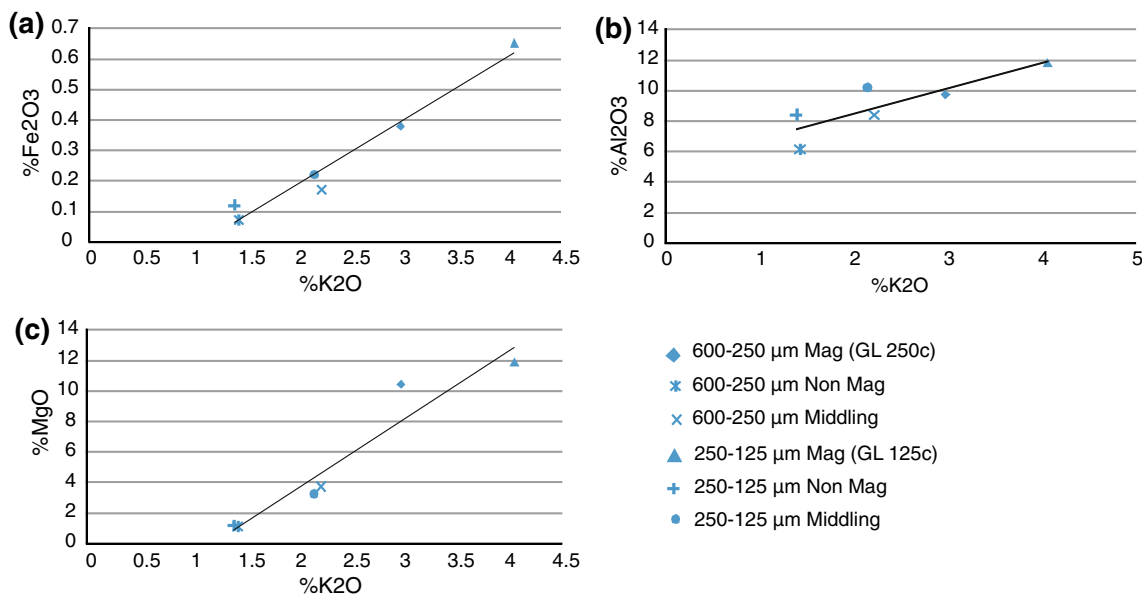
Fig. 4. Correlation curves for K_2O and **a** Fe_2O_3, **b** Al_2O_3, and **c** MgO.

liberation from GL250c was more effective in the first 15 days but started to decrease whereas K-liberation from GL125c continued to increase. This probably had to do with higher K-content in GL125c, 36 % higher than GL250c. Specific area changes could also have influenced liberation rate mentioned before.

According to agronomic assays, fertilization efficiency was very similar using either GL250c or GL125c (Fig. 7). Seedlings fertilized by GL250c and GL125c showed 109 and 97 % more ashes of accumulated biomass when compared to that of the control sample. Although KCl fertilization gave greater yields during the first four harvests, samples fertilized with GL250c and GL125c showed an increase in 10 and 4 %, respectively, after overall harvests. This behavior is probably a response to early fast K-liberation from the salt (KCl) in contrast to slow release K-liberation from glauconitic pellets.

The K-content of biomass ashes (Fig. 7) started to be significant, compared to that of the control
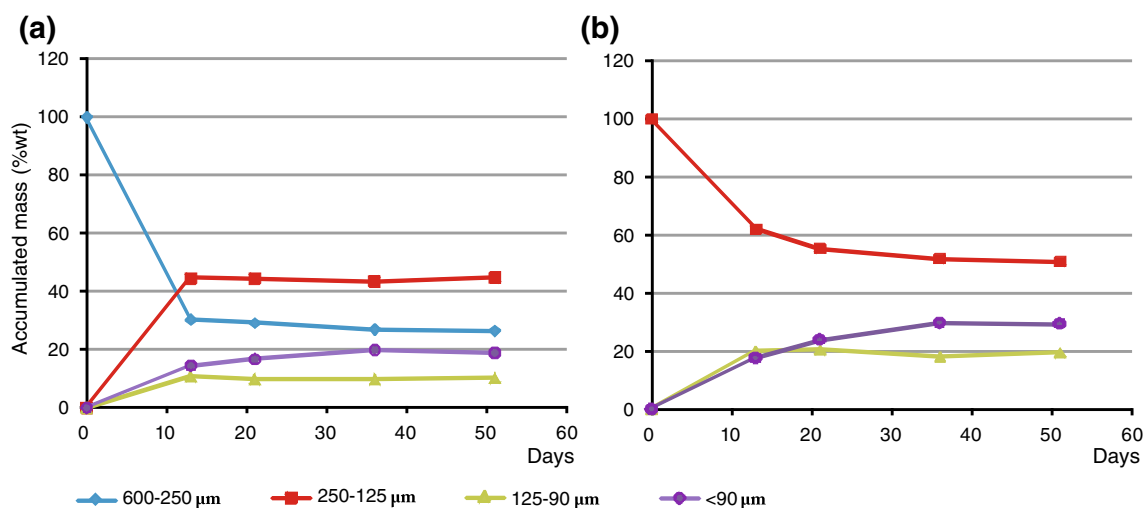
(a)

(b)

● 600-250 μm ■ 250-125 μm ▲ 125-90 μm ● <90 μm

Fig. 5. Granulometric changes through lixiviation tests on **a** GL250c and **b** GL125c.
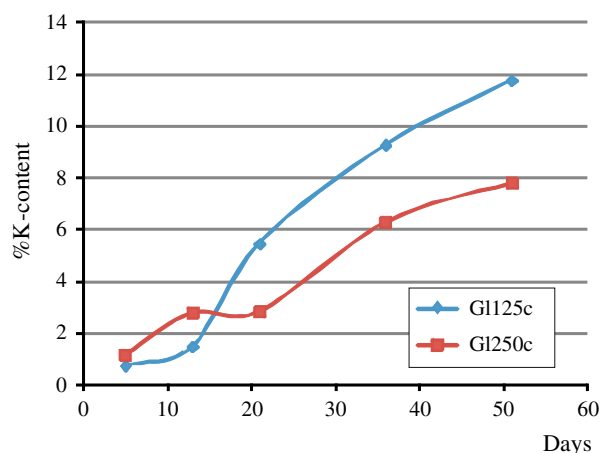
Fig. 6. Curves for K extraction for GL250c and GL125c during lixiviation tests.

Fig. 7. Accumulated weight of biomass ashes (after calcination at 550 °C) versus number of harvest for KCl, GL125c, GL250c, and control sample from agronomic assays.

samples, since the second harvest for all samples probably due to crop's characteristics. KCl released important amounts of K specifically in the second harvest but decreased in the following ones and continued to do so with respect to GL250c and GL125c in the succeeding harvests. In contrast, glauconitic samples released less K during the second harvest but started to supply more in the following ones, reaching K level from KCl in the fourth harvest and over passing it in the fifth harvest. However, GL250c started to release slightly more potassium earlier than GL125c probably as a consequence of higher specific surface and micropores (Table 4). In the fourth harvest, this relation
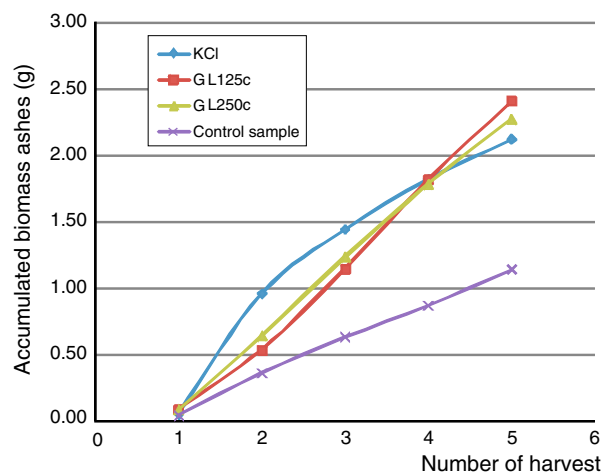
changed as GL125c started to release slightly more potassium than GL250; this is likely a response to its higher potassium content and to its relative higher change in specific area as mentioned before. These indicate that absolute lower specific area and micropores values of GL125c would be compensated by both major relative change in specific area and its K-content that is 36 % higher than that of GL250c. In other words, the lower specific area but higher K-content of the GL125c is equivalent to the higher specific area and micropores but lower K-content of GL250c, as similar agronomic efficiency is finally reached using either sample.

Table 4. Specific surface area and micropores for GL250c and GL125c before and after leaching

Samples	Specific surface (m²/g)	Micropores area (m²/g)	% Micropores
GL250c			
Initial	30.32	7.35	24.24
After leaching	35.25	6.3	17.88
GL125c			
Initial	22.28	3.47	15.57
After leaching	28.23	3.54	12.54

Table 5. K_2O wt% per fertilizer (KCl, GL125c and GL250c) and its equivalent to 1 t of KCl

Fertilizers	K_2O wt%	K_2O kg/t	t equivalent to 1 t of KCl
GL125c	4.05	40.5	15.63
GL250c	2.97	29.7	21.31
KCl	63.3	633	1.00

Economic Considerations

As mentioned before, greensands from the Salamanca Formation are found loosely or poorly consolidated at or near the surface with little or no overburden. Castro and Soreda (2009) inferred 2,800 Mt of resource. It is necessary to consider the significant influence that haulage costs could have on the final prize of glauconitic fertilizers considering the amount of concentrated greensands (GL250c and GL125c) required to obtain similar results as when using KCl (Table 5). Therefore, it is recommended to restrict the use of this alternative fertilizer to near exploitation areas. Therefore, Patagonia seems to be a proper exploitation area as there are many small scale organic crop activities specially related to different kinds of berries that could work as potential demand markets close to the Salamanca Formation deposits.

CONCLUSIONS

GL250c (4.05 % K_2O) and GL125c (2.97 % K_2O) gave similar yields after overall harvests and slightly higher yields compared to KCl-fertilized sample. Therefore, magnetically concentrated greensands from the Salamanca Formation showed to be an alternative K-fertilizer compared to KCl. As similar results were obtained using either GL250c or GL125c, sieving process to obtain these fractions is not necessary and would only add extra cost in production. The advantage of these sands if mined is that they are naturally loose to poorly compact, and thus, no significant grinding would be required. Furthermore, these sands are found at or near the surface with little or no overburden. Simple magnetic separation treatments as dry high intensity magnetic separator would be enough for obtaining a competitive alternative K-fertilizer with the advantage of lacks in Cl preventing salinization of soil. Greensands from the Salamanca Formation seem to be an effective slow release alternative source of K-fertilizers with potentially low cost production and treatment compared to operation costs for mining potassium soluble salts at depth. Nevertheless, haulage costs for potential fertilizer product from these sands could have significant influence in final prize. Therefore, its commercialization should be restricted to near glauconitic deposits. Accordingly, Patagonia seems to be a proper place for exploiting these types of deposits.

REFERENCES

Abd El Rahman, M. K. (2006). Degritting of glauconite clay by different techniques for use in water treatment and as fertilizer. *Mineral Processing and Extractive Metallurgy, 116*(8), 145–149.

Amazons Cerrado Verde Potash Project. (2012). A potash solution for Brasil's growing potash problem. http://www.amazonplc.com.

Amorosi, A. (1995). Glaucony and sequence stratigraphy: A conceptual framework of distribution in siliciclastic sequences. *Journal of Sedimentary Research, 65*, 419–425.

Amorosi, A. (1997). Detecting compositional spatial and temporal attributes of Glaucony: A tool for provenance research. *Sedimentary Geology Journal, 109*, 35–153.

Amorosi, A., & Centineo, M. C. (1997). Glaucony from the Eocene of the Isle of Wight (southern UK): Implications for basin analysis and sequence-stratigraphic interpretation. *Journal of the Geological Society, 154*, 887–896.

Banerjee, S., Eevankumar, S., & Riksson, P. G. (2008). Mg-rich illite in marine transgressive and high stand system tracts: Examples from the Palaeoproterozoic Semri Group, Central India. *Precambrian Research, 162*, 212–226.

Castro, L. N., Fazio, A. M., Scasso, R. A., Tourn, S., & Soreda, M. E. (2008). Potential potassium deposits in Patagonia. Southeast of Argentina. Bulletin of the Tethys Geological Society (Bull. T.G.S.). *Proceeding of Third International Conference on the Geology of the Tethys, 3*, 275–280.

Castro, L. N., Scasso, R. A., Branzini, A., Zubillaga, M. S., Fazio, A. M., Tourn, S. M., et al. (2010). Los niveles glauconíticos de la Formación Salamanca. Chubut: su efectividad agronómica como fuente alternativa de fertilizante potásico de liberación controlada. *Revista de la Asociación Geológica Argentina, 66*(3), 391–398.

Castro, L. N., & Soreda, M. E. (2009). Evaluación de los niveles glauconíticos en la Formación Salamanca como recurso minero de aplicación industrial, Paleoceno inferior de la cuenca del Golfo de San Jorge, provincias de Chubut y Santa Cruz. *Proceeding of 9° Congreso Argentino Geología Económica, 1*, 159–164.

Castro, L., & Tourn, S. (2004). Direct application of phosphate rocks and glauconite as alternative sources of fertilizer in Argentina. SUM 21 special issue of Exploration and Mining Geology on sustainable development in the minerals industry. Geological Society of Canadian Institute of Mining. *Metallurgy and Petroleum, 12*, 72–79.

Chattoraj, S. L., Banerjee, A., & Saraswati, P. K. (2009). Glauconites from the Late Palaeocene–Early Eocene Naredi Formation, western Kutch and their genetic implications. *Journal of the Geological Society of India, 73*, 567–574.

Coles, S. K., Wright, C. I., Sinclair, D. A., & Van den Bossche, P. (2002). The potential for environmentally sound development of marine deposits of potassic and phosphatic minerals offshore, southern Africa. *Marine Georesources and Geotechnology, 20*(2), 87–110.

Dooley, J. H. (2006). Glauconite. In J. Koger, N. Trivedi, J. Barrer, & N. Krukowsky (Eds.), *Industrial minerals and rocks: Commodities, market and uses* (pp. 495–506). Littleton, CO: Society for Mining, Metallurgy and Exploration.

Folk, R. L., & Ward, W. C. (1957). Brazos River bar: A study in the significance of grain size parameters. *Journal of Sedimentary Petrology, 27*, 3–26.

Franzosi, C. (2009). Geología y evaluación de los recursos mineros para la agricultura del área del cerro Tortuga, Provincia del Chubut, Argentina. Final Geologist Grade Thesis, University of Buenos Aires (unpublished).

Hao, O. J., & Tsai, C. M. (1987). The removal of metals and ammonium by natural glauconite. *Environment International, 13*(2), 203–212.

Hassan, M., & El-Shall, H. (2004). Glauconitic clay of El Gidida, Egypt: Evaluation and surface modification. *Applied Clay Science, 27*, 219–222.

Heffer, P., & Prud'homme, M. (2013). Fertilizer outlook 2013–2017. In *81st IFA Annual Conference*, Chicago, May 2013. http://www.fertilizer.org/HomePage/FERTILIZERS-THE-INDUSTRY/Market.

Kitamura, A. (1998). Glaucony and carbonate grains as indicators of the condensed section: Omma Formation, Japan. *Sedimentary Geology Journal, 122*, 151–163.

Levchenko, E., Patyk-Kara, N., & Levchenko, M. (2008). Glauconite deposits of Russia: Perspectives of development. MRD-07 Geology and mineral potential of CIS countries. In *33° International Geological Congress*, Oslo. Abstract. http//:www.cprm.gov.br/33IGC/1259055.html.

Loveland, P. J. (1981). Weathering of a soil glauconite in Southern England. *Geoderma, 25*(1–2), 35–54.

McManus, J. (1988). Grain size determination and interpretation. In M. Tucker (Ed.), *Techniques in sedimentology* (pp. 63–85). Oxford: Blackwell.

McRae, S. G. (1972). Glauconite. *Earth Science Reviews, 8*(4), 397–440.

Odin, G. S., & Matter, A. (1981). De Glauconiarum Origine. *Sedimentology, 28*, 641–644.

Potash. (2012). *Commodity statistics and information*. United State Geological Survey. http://minerals.usgs.gov/minerals/pubs/commodity/potash/mcs-2012-potas.pdf.

Srasra, E., & Trabelsi-Ayedi, M. (2000). Textural properties of acid activated glauconite. *Applied Clay Science, 17*, 71–84.

TIFAC. (2009). *Technologies for agricultural application of glauconite—A potash mineral*. http://www.tifac.org.in/.

Tourn, S., Castro, L., Celeda, A., Scasso, R., Fazio, A., & Soreda, M. E. (2008). Mineralogía y geoquímica de las glauconías de la Formación Salamanca, Chubut, Argentina. *Proceeding of 17° Congreso Geológico Argentino, Jujuy, 3*, 910–912.

Wentworth, C. K. (1922). A scale of grade and class terms for clastic sediments. *Journal of Geology, 30*, 377–392.